THE MARSHALL AUTOMATED WIND ALGORITHM: ERROR ANALYSIS, QUALITY CONTROL AND CLIMATE APPLICATIONS

Gary J. Jedlovec (NASA) and Robert J. Atkinson (Lockheed Martin)
Global Hydrology and Climate Center, 977 Explorer Blvd.
Huntsville, AL USA 35806

ABSTRACT

The Marshall Automated Wind (MAW) algorithm for wind determination from geostationary satellite data is described and contrasted with other methods. The major differences between the MAW technique and others are found in the target selection, template size, search area constraints, and in the quality control procedures. Using appropriate data dependent tracking parameters and quality controls, random wind errors are held to around 3.0 ms^{-1} as estimated with structure function analysis. It is shown that structure function analysis is also a useful tool to monitor the reduction in wind errors as a result of tracking procedure improvements. A tracking error parameter is developed to provide guidance for the trade-offs between spatial and temporal resolution when rapid scan satellite imagery is used. Major sources of error implicit in wind tracking are discussed.

1. INTRODUCTION

The standard approach taken in generating wind fields from geostationary satellite data uses a sequence of two or more images to track identifiable image features (determine image displacements). There has been considerable research into developing the optimum tracking algorithms for this purpose, much of which has been documented in previous wind workshops and also in the peer-reviewed literature. In this paper, we document a technique which is similar to the approach taken by NESDIS for their operational applications (Velden et al. 1997, and Neiman et al. 1997) but incorporates features (different template sizes, search conditions, and quality controls) which may improve the wind determination under particular situations. The Marshall Automated Wind (MAW) technique was initially developed over 15 years ago in support of NASA mesoscale wind studies and has been refined over the years and is now used as a climate analysis tool and to provide validation datasets for future wind sensor studies. An assessment of the errors in the winds derived from the MAW is made using structure function analysis which does not rely on *a priori* information or rawinsonde data for comparison. We also present a comprehensive discussion on the source of errors in cloud- and water vapor-tracked winds and how the methodology used in the MAW algorithm minimizes these problems.

2. TRACKING METHODS

The basic approach of all satellite wind tracking schemes is the *identification* of features common (in time) to a sequence of images and the *determination of their relative positions* with respect to

some fixed coordinate system. The latter is accomplished by using accurate navigation of the individual satellite images and a conversion of displacement in satellite coordinates to that of earth coordinates. This procedure is well established. The former problem (feature identification) is not a trivial issue and is compounded by relatively poor satellite resolution of clouds and water vapor features and the changing dynamical environment which governs cloud development and the movement of water vapor in the atmosphere. Originally this task was done with the concept of the "man-in-the-loop" whereby the human, with superior ability to visually identify and track features, views a sequence of images to accurately identify and determine physical displacements of clouds in the imagery (Stewart et al. 1985). This process is highly accurate because the human can also use his knowledge and experience of atmospheric processes to determine the proper features to track. This process is quite labor intensive and not applicable to the generation of large wind datasets for research or operational applications. There are a number of automated approaches to feature identification between a pair of images (e.g., Endlich et al. 1981; Eigenwillig and Fischer 1982). Soden (1998) has developed an approach that uses a time-lagged cross correlation method on a sequence of two GOES VAS water vapor images separated by 60 minutes. Reverse correlation (tracking features in the second [later in time] image to the first image) is used to provide confidence in the retrieved wind vector. Laurent (1993) used a cross correlation method with a sequence of three Meteosat 5 images separated by 30 minutes with vector pair checks used for determining good wind vectors. Velden et al. (1997) and Neiman et al. (1997) described the approach used by NOAA/NESDIS for both operational support and research applications. Their approach uses the sum of the squared differences between the target box and a search box in a sequence of three water vapor images separated by 30 minutes in time. Vector pair consistency checks and automated editing procedures based on model forecasts are used in quality and control procedures. The MAW approach is similar to that used by NESDIS, but just the sum of the difference between pixels in a tracking template from image to image provides the feature matching between sequential images. These algorithms differ in other ways as well; namely, in their use of template size, search area, target selection, and editing procedures which can produce differences in the accuracy and resolution of the derived wind vectors.

3. MARSHALL AUTOMATED WIND TECHNIQUE

Early versions of the MAW algorithm have been documented in Atkinson (1984, 1987). The discussion below describes the current version of the MAW algorithm which has been used to study the upper-level water vapor transport associated with the 1987/1988 ENSO period and is now being applied to investigate water vapor transport during the 1997-1998 ENSO event. The algorithm uses a minimum-difference template matching scheme for feature identification and tracking. In the tracking procedure, the first of a pair of images is divided into image sub-scenes called templates, while the second image contains sub-scenes called search areas (Figure 1). The template (T^1) is an array of picture elements and the spatial location of a template is designated as the template's center picture element location in the image (e.g., i,j). The initial target regions are uniformly spaced throughout the image. To determine feature displacement or motion (winds), each template, $T^1_{i,j}$, in image 1 is translated to all possible positions within a corresponding search area, $S^2_{i,j}$, in the second image looking for the best match. The best match is simply the position of the template, $T^2_{i+x,j+y}$, in image 2 which, when differenced with the original template position in image 1, gives the smallest mean difference value. Once the best match is found, its position within the search area (i+x,j+y) along with its initial position in image 1 determine the template displacement (D) between the two images (x,y) in satellite coordinates. Accurate navigation and registration of the two images allows for the determination of displacement or velocity vectors relative to the Earth (u and v components of the wind). The MAW approach is optimized when a sequence of three images is used to derive two vectors (displacement of feature from image 1 to image 2, and displacement of the same feature from image 2 to image 3) for the movement of each feature (Figure 1). The vector pairs ($\mathbf{V_1}$ and $\mathbf{V_2}$) are used in quality checks as discussed below, and the average of the two vectors is used as the final estimate of the wind over the template region. A

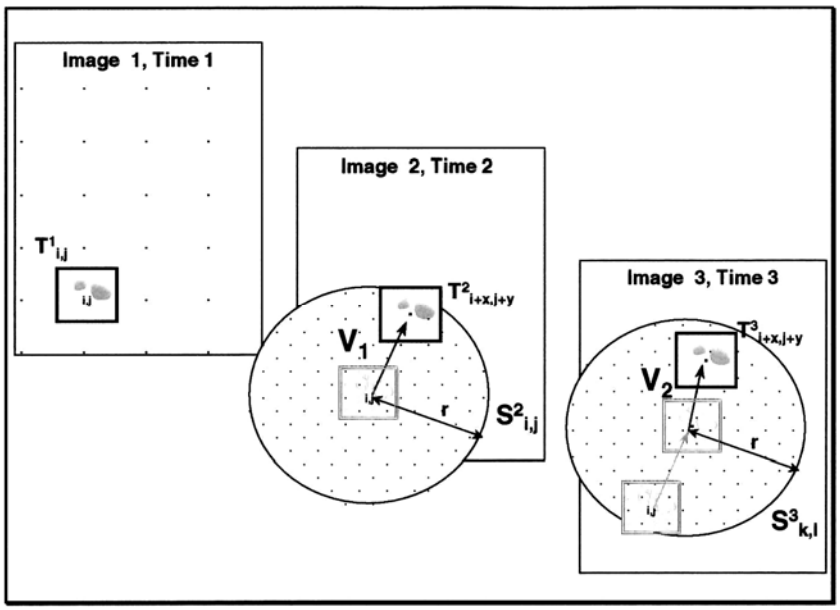

Figure 1. Feature identification and tracking approach used in the MAW technique.

pressure-height is assigned to the wind based on referencing the mean brightness temperature over the template to a local thermodynamic profile.

When using the MAW tracking scheme, there are several decisions to be made that affect the quality of the resulting motion vectors (winds): image spatial and temporal resolution, template size, and search constraints. Experience indicates that the highest quality winds come from the appropriate match of spatial and temporal resolution. Merrill (1989) and Schmetz et al. (1993) have discussed the effect of image resolution on the ability to track image features. Use of high temporal resolution data with coarse spatial resolution produces poor winds because the pixel displacement of the feature is small, in which case navigation and registration uncertainties heavily influence the results. This is visualized with the development of the Tracking Error Lower Limit or TELL. The TELL indicates the appropriate (actually minimum) image separation time for a given spatial resolution of satellite data to keep image registration errors from dominating the results. The TELL (ms^{-1}) is expressed as the product of the image spatial resolution (X) and the image-to-image registration accuracy (Z) divided by the image temporal resolution (Y). The lower limit on the wind accuracy is a function of how well the data can detect small movements in features in the satellite imagery which is a function of these three parameters. For a given set of X, Y, and Z values, a family of curves can be generated that describe the lower limit on the expected wind accuracy. The chart of this is presented in Figure 2. For an assumed image-to-image registration of 0.25 pixels typical for GOES 8/9/10 (Graumann 1998), a family of curves can be generated and are shown for various image separation times. It can be seen that for 8 km image data (e.g., for GOES 8/9/10 water vapor imagery), the TELL is less than 2.0 ms^{-1} for image separations of greater than 15 minutes. As smaller temporal separations are used, the imagery is unable to resolve small movements in cloud or water vapor features because of the relatively course resolution of the image data. For 4 km data, temporal separation of about 7-8 minutes can be used to resolve winds with an accuracy down to 2.0 ms^{-1}. The chart can be used another way as well. For example, for 1 minute imagery and 1 km spatial resolution image data, wind errors will likely exceed 4.0 ms^{-1} due to feature location uncertainty alone. Obviously these curves will change as the assumed image-to-image registration accuracy is changed. Thus the bottom line is that there is a limit to the use of finer temporal resolution without increased image resolution. This trade-off impacts the accuracy of the winds. On the other hand, large temporal sampling may introduce errors in tracking because of the evolution and subsequent de-correlation of features between image times. This problem is dependent on the particular application and scale of the features being tracked, both of which are difficult to quantify.

An example of water vapor winds derived from applying the MAW algorithm to a sequence of GOES 9 images for February 22, 1998 is presented in Figure 3. Three images (8 x 4 km resolution) were used with a 15 x 55 pixel tracking template (square in earth coordinates because of pixel sampling and overlap). The initial positions of the tracking template were selected as regular gridpoints with a spacing of about 120 km. This provided near-contiguous spatial coverage without template overlap. A circular search area of 225 km allowed for a maximum wind of 75 ms^{-1} (which increases away from nadir). The use of three images allows for the calculation of two vectors corresponding to each feature. The average of the two vectors for each location is plotted in the figure. The initial distribution of wind vectors is quite uniform (by design) and the winds show good spatial consistency in most areas.

The calculation of two wind vectors per feature is quite common in both research and operational processing of satellite data (Nieman et al. 1997; Velden et al 1997; Laurent 1993; Schmetz et al. 1993) and it allows for continuity or symmetry checks between the vector pairs. Speed differences between vector 1 and vector 2 at a given location greater than 10 ms^{-1} or direction differences greater than 20° serve as the primary quality control on the MAW winds in this instance. Jedlovec et al. (1998) used 15 ms^{-1} and 30 ° respectively for GOES VAS data. This approach is a bit different from the operational scheme of NESDIS (Nieman et al. 1997) where a 5 ms^{-1} u and v vector pair threshold is the primary filter on bad winds (although additional automated procedures are also used). Our approach is less restrictive in that it allows larger deviations, and flags (as bad) vector pairs which show totally different flow characteristics (large direction differences between vector pairs). Vector pairs which show considerable agreement are averaged together to form a single vector valid at the middle image time and assigned a location on Earth based on the average displacement of the two vectors. Figure 3 shows both the good winds and the bad winds (those which failed the above speed and direction checks). It is quite apparent that the bad winds (red wind flags) are spatially inconsistent with many of their neighbors. These bad vectors occur throughout the image but are more prevalent in non-cloud regions of the water vapor imagery. The errors probably result from 1) lack of trackable image structure, 2) significant changes in image structure over the 2-hour tracking sequence, or 3) multiple solutions in the matching approach. There are many good wind vectors (yellow) throughout the image which show consistent flow patterns associated with outflow from tropical convective systems, strong winds associated with synoptic systems in both hemispheres, and large-scale flow characteristics winds away from convective regions.

4. WIND ERRORS

In the application of tracking algorithms to sequential satellite imagery for wind determination, it is assumed that the clouds or water vapor features are conservative, passive tracers of the wind field. However, this is not always the case and changes in shape and radiative characteristics of clouds and water vapor features may be mis-interpreted and lead to wind errors. Velden et al (1997) recognized this and provides an explicit correction to the wind vectors to account for a consistent slow bias when compared to the model forecast of winds. Wind vectors can also be in error as a result of mis-identification of targets from scene-to-scene and from improper determination of correct image displacements. The latter arises from inaccurate image navigation and registration between image scenes and usually results as a bias in all vectors. This mis-registration can be identified and corrected when it occurs by tracking discernable surface features in the visible or infrared window channel imagery.

The magnitude of the error implicit in satellite derived winds is, at times, difficult to assess because of the lack of ground truth or verification data. There is a tendency to compare satellite-derived winds to rawinsonde winds to assess their accuracy. While rawinsondes provide a traditional standard for ground truth comparisons of many satellite-derived products (temperature and moisture profiles, total precipitable water vapor, winds, etc.), care must be used in interpreting the

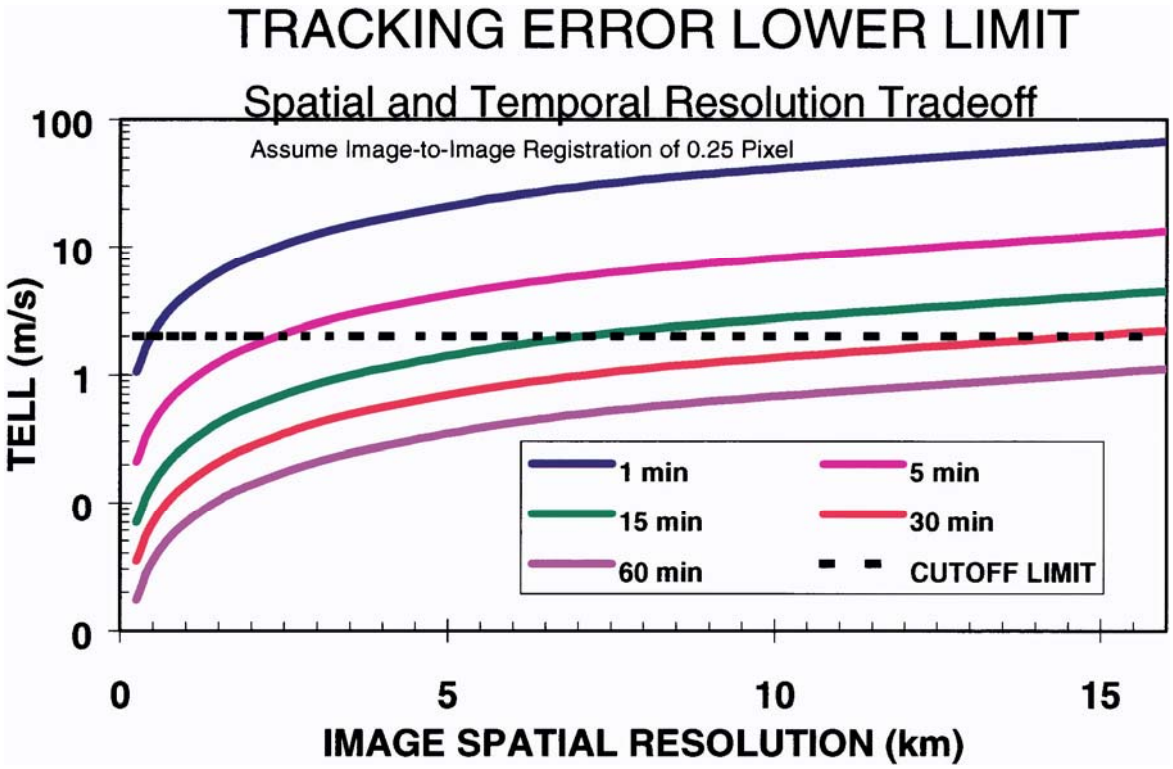

Figure 2. The Tracking Error Lower Limit (TELL) curves in the diagram above provide a mechanism to assess the effect of image spatial resolution and temporal separation on tracking accuracy.

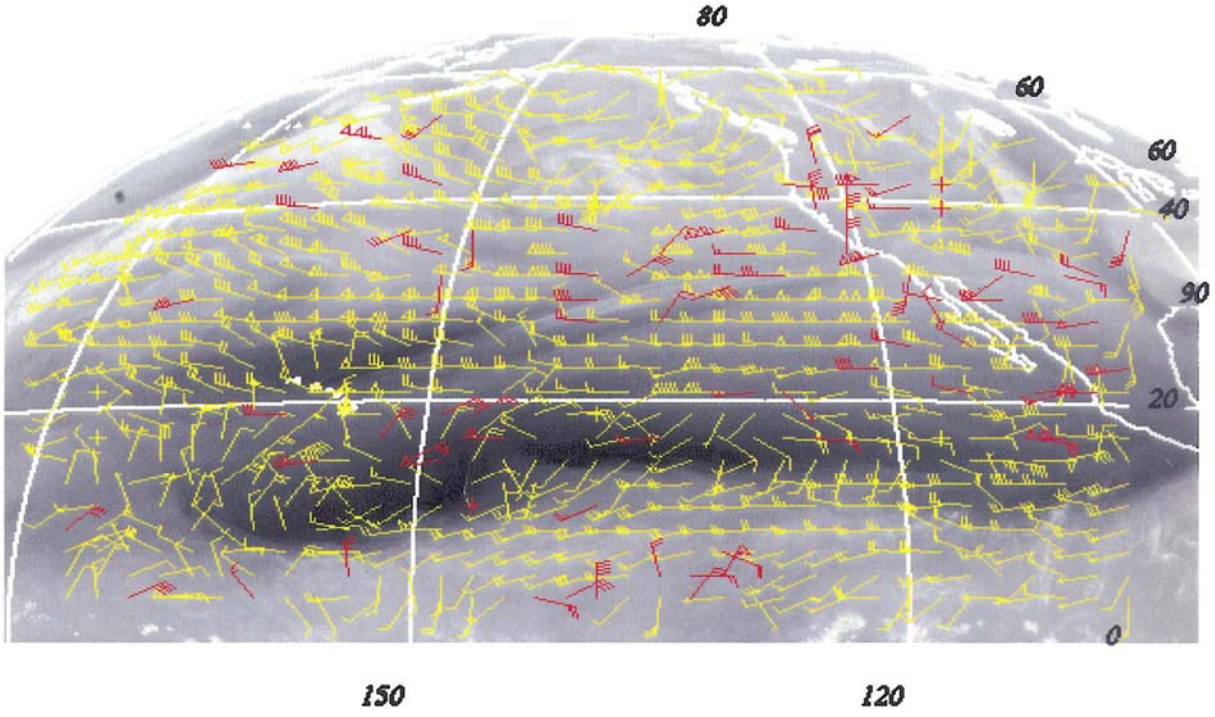

Figure 3. Upper-tropospheric water vapor-tracked winds from the GOES 9 satellite using the MAW algorithm. Winds exceeding a 10 ms^{-1} speed deviation and a 20° direction deviation are plotted in red along with the good wind vectors in yellow. Spacing of the winds is about 120 km.

results of such comparisons for winds. The rawinsondes are essentially a point measurement at a specific time and have their own error sources. Satellite-derived winds are a volumetric (vertical and horizontal) estimate of the flow characteristics averaged or sampled over a period of time (anywhere from a few minutes to hours). These comparisons (to rawinsonde data) can only provide limited guidance on the accuracy of satellite derived winds. A somewhat unique approach to error assessment in satellite-derived winds is the use of statistical structure function analysis to independently quantify the *random error* associated with the wind dataset without reference to rawinsonde or modeled wind data. Hillger and Vonder Haar (1988) and Fuelberg and Meyer (1986) and others have shown that structure function analysis can be used to estimate the magnitude of mean non-direction gradients (structure) in data fields. The value of the structure curves at small separation intervals can be used in the error estimation. Structure function analysis was used to estimate the random error in the water vapor winds shown in Figure 3. When all the winds are considered, the error was determined to be 7.4 ms^{-1}. When the quality control thresholds (vector pair differences of 10 ms^{-1} in speed or 20° direction) are considered, random errors are reduced to 3.4 ms^{-1} . The reduction in this random error associated with the use of editing procedures is used as a measure of success for the quality and control parameters.

One of the key parameters in the MAW approach is the template size. The template defines a region in the image which contains the pattern to be matched. Laurent (1993) used a 32 x 32 pixel (25,600 km^2) region in 5 km Meteosat 5 data while Soden (1998) used a region equivalent to 46 x 46 pixels (135,424 km^2) in 8 km *GOES-7* data. Neiman et al. (1997) and Velden et al. (1997) use a 15 x 15 pixel (2160 km^2) region in 4 km *GOES-8* data. Not only is the template quite small, but the template shape (footprint on ground) is rectangular because of sensor fov overlap. This biases search conditions and template matching. Jedlovec et al. (1998) used a 49 x 49 pixel template (153,664 km^2) with GOES VAS data. The large templates with GOES VAS were necessary because of the coarse sensor resolution (actually 16 x 16 km) and poor radiometric quality of the data. Our current work with GOES 8/9/10 varies between a 13-15 x 45-55 pixel (7406 km^2) square (on the ground) template which is three times the size Velden et al. (1997) used for GOES 8 data. If the template is too small, the pattern or structure of the water vapor field is quite uniform, making a successful match in the second or subsequent images difficult to accurately obtain. In order to determine the best template size, one can examine the spatial structure in the GOES imagery. This has been explored to some degree in the past by Jedlovec and Atkinson (1996). In the absence of clouds, the upper-tropospheric water vapor structure is quite limited, with significant gradients observed only at scales greater than several hundred kilometers. The presence of high clouds adds significant structure to the imagery at scales below this threshold.

Another way to determine the appropriate template size for feature tracking is to demonstrate the relationship between accuracy of the winds and template size. To show this, the MAW scheme was used to track features in GOES water vapor imagery with varying template size. The results are shown in Figure 4 for *GOES-8* imager data. The random noise present in the derived wind vectors for each run was determined with structure function analysis. It is obvious from the figure that large wind errors are associated with small templates. Jedlovec and Atkinson (1996) showed a similar curve for GOES VAS data. The noise is lower in the *GOES-8* data because of better sensor resolution (nominally 16 x 16 km for VAS and 8 x 8 km for *GOES-8* imager) and radiometric precision of the data. Significant errors occur at small templates because there is ambiguity in matching small features (structure in small templates) over a given time interval. There is some indication that a geometrically square (on the ground) template does better than a similar size rectangular one. The random noise decreases with increasing template size as the larger template detects more image structure. The approximate node point in the curve where random wind errors no longer change rapidly with template size is about 25 x 45 pixels for GOES 8 data. Previous work has shown that a template size of 49 x 49 - 8 km pixels is appropriate for the older GOES VAS data which is consistent with the template size used by Soden (1998) and Jedlovec et al. (1998). For GOES 8 data, random wind errors for typical templates range from 3-8 ms^{-1} for unedited data (with no post processing quality control). Smaller templates may be appropriate for cloud tracking where

thermal (infrared) or reflectance (visible) image structure is greater than that of the water vapor imagery or in regions of the water vapor imagery where high clouds dominate. The use of quality control procedures to reduce the errors in the data has an interesting effect on the noise versus template size relationship. Noise can be significantly reduced for all template sizes with the use of appropriate quality controls. In Figure 4, the thin, long-dashed curves corresponded to the use of a 5 ms^{-1} acceleration criteria (typical for NESDIS operations) between two vector pairs. For this situation, random noise is estimated at between 2-4 ms^{-1} for all template sizes. As can be seen by the small dashed lines (right axis), the number of good vectors (those passing quality controls) is substantially reduced (by as much as 50-75% for NESDIS operations) as a result of the quality controls.

Another tracking algorithm parameter which can induce errors in the winds if not properly selected is the size of the search area. The search area size (and shape) should be influenced by the expected magnitude and direction of the wind. Use of too large a search area may allow erroneous matches which produce unrealistic wind displacements. Very small search areas artificially constrain the winds and reduce the number of good matches in the search area.

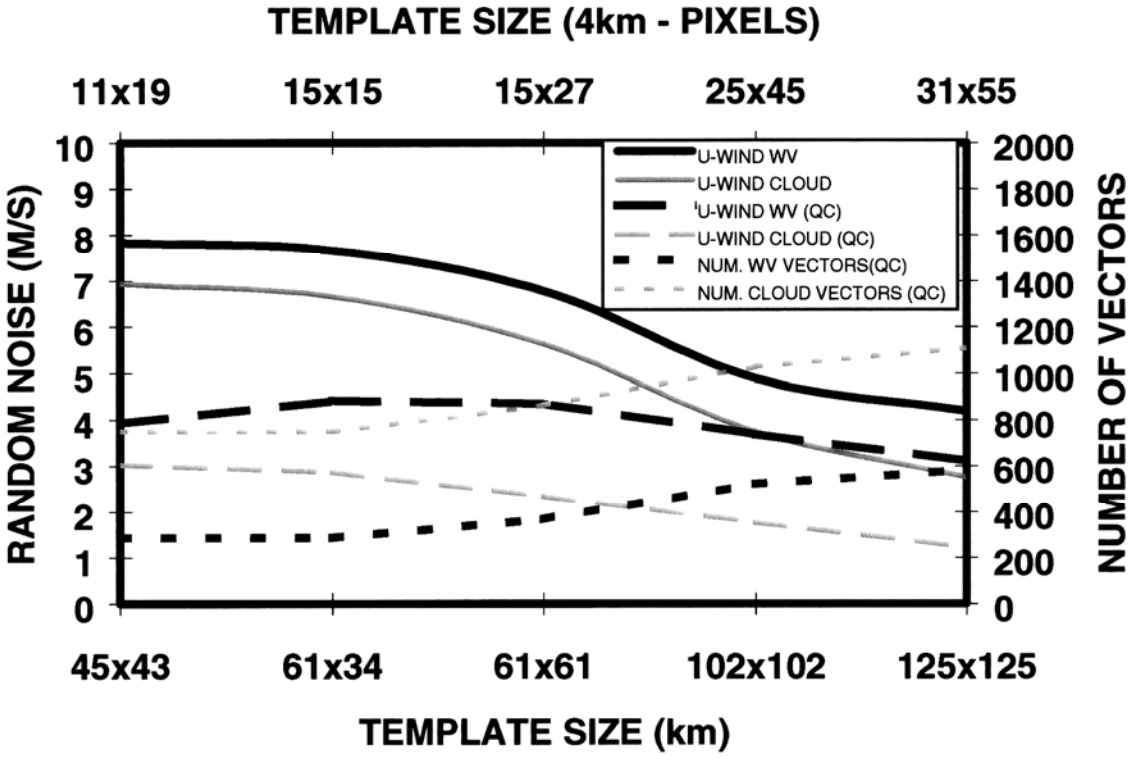

Figure 4. Random noise in wind datasets as a function of tracking template size.

Velden et al. (1997), Neiman et al. (1997), and Schmetz et al. (1993) have used winds from a numerical model to provide a first guess location of the image displacement (wind) to center a search and to potentially reduce computation time. This is helpful if computer time is important (operational constraints) and if the user is confident that the "guess" is reasonable. While limiting the search area to some reasonable size (based upon maximum expected wind) is prudent, our experience has shown that in regions where winds are poorly represented in model forecast fields (such as tropical ocean regions), use of a model guess could force the wind retrieval algorithm to look in the wrong place for a match. In the performance analysis of MAW algorithm, the rejection of a large number of wind vectors because the template difference is on the edge of the search area is an indication of too small a search area or limited image structure. In our evaluation of the NESDIS

operational wind algorithm (Jedlovec and Atkinson 1997) 10-12% of the initial targets were rejected because matches were found on the edge of the search area. In our current applications to GOES 8/9/10 data, the search distance is selected based on image resolution and temporal separation such that speeds up to 75 ms^{-1} can be detected. No guess is used to influence the position of the search area. Recent work has also shown that utilizing a smaller search area in subtropical high pressure regions where winds are light reduces the number of bad vectors by reducing the possibility of erroneous matches. The implementation of a scheme which varies search radius or distance over the image is being considered for the MAW algorithm.

REFERENCES

Atkinson, R. J. 1984: Automated mesoscale winds determined from satellite imagery. Interim Report on NAS8-34596, General Electric Company, Huntsville, AL, 51 pp.

__ , 1987: Automated mesoscale winds determined from satellite imagery. Final Report on NAS8-34596, General Electric Company, Huntsville, AL, 50pp.

Eigenwillig, N. and H. Fischer, 1982: Determination of mid-tropospheric wind vectors by tracking pure water vapor structures in METEOSAT water vapor image sequences. *Bull. Amer. Meteor. Soc.,* **63,** 44-58.

Endlich, R.M. and D.E. Wolf, 1981: Automatic cloud tracking applied to GOES and METEOSAT observations. *J. Appl. Meteor.,* **20**, 309-319.

Fuelberg, H. E. and P.J. Meyer, 1986: An analysis of the AVE-SESAME I period using statistical structure and correlation functions. *Mon. Wea. Rev.,* **112,** 1562-1576.

Graumann, A. (editor), 1998: GOES data user's guide. U.S. Department of Commerce, NESDIS, NCDC, Asheville, NC, 190 pgs.

Hillger, D.W. and T.H. Vonder Haar, 1988: Estimating noise levels of remotely sensed measurements from satellites using spatial structure analysis. *J. Atmos. Oceanic Technol.,* **5**, 206-214.

Jedlovec, G. J., and R. J. Atkinson, 1996: Quality and control of water vapor winds. *Proc. Eighth Conference on Satellite Meteorology and Oceanography,* Atlanta, Amer. Meteor. Soc., 5-8.

Jedlovec, G. J., J. A. Lerner, and R. J. Atkinson, 1998: A satellite-derived upper-tropospheric water vapor transport index for climate studies. Submitted to *J. Appl. Meteor.,* July 1998.

Jedlovec, G. J., and R. J. Atkinson, 1997: Error analysis of NESDIS water vapor winds. Interim report to the GIMPAP Committee, September, 1997.

Laurent, H. 1993: Wind extraction from Meteosat water vapor channel image data. *J. Appl. Meteor.,* **32,** 1124-1133.

Merrill, R. T., 1989: Advances in the automated production of wind estimates from geostationary satellite imagery. *Preprints, Fourth Conf. On Satellite Meteorology and Oceanography,* San Diego, Amer. Meteor. Soc., 246-249.

Neiman, S.J., W.P. Menzel, C.M. Hayden, D. Gray, S.T. Wanzong, C.S. Velden, and J. Daniels, 1997: Fully automated cloud-drift winds in NESDIS operations. *Bull. Amer. Meteor. Soc.,* **78**,1121-1133.

Schmetz, J., K. Holmlund, B. Hoffman, B. Mason, V. Gaertner, A. Koch, and L. Van de Berg, 1993: Operational cloud-motion winds from Meteosat infrared images. *J. Appl. Meteor.,* **32,** 1206-1225.

Soden, B.J. 1998: Tracking upper tropospheric water vapor radiances from satellite. *J. Geophys. Res. (accepted).*

Stewart, T.R., C.M. Hayden, and W.L. Smith, 1985: A note on water-vapor wind tracking using VAS data on McIDAS. *Bull. Amer. Meteor. Soc.,* **66**, 1111-1115.

Velden, C., C. M. Hayden, S. J. Nieman, W. P. Menzel, S. Wanzong, and J. S. Goerss, 1997: Upper-tropospheric winds derived from Geostationary satellite water vapor observations. *Bull. Amer. Meteor. Soc.,* **78,** 173-195.